

RESEARCH

Open Access



# hsa\_circ\_0007919 induces LIG1 transcription by binding to FOXA1/TET1 to enhance the DNA damage response and promote gemcitabine resistance in pancreatic ductal adenocarcinoma

Lei Xu<sup>1,2,3†</sup>, Xiao Ma<sup>1,2,4†</sup>, Xiuzhong Zhang<sup>1†</sup>, Chong Zhang<sup>1</sup>, Yi Zhang<sup>1</sup>, Shuai Gong<sup>1</sup>, Nai Wu<sup>1</sup>, Peng Zhang<sup>1,2,5</sup>, Xinyu Feng<sup>1,2</sup>, Jiaxuan Guo<sup>1,2</sup>, Mengmeng Zhao<sup>1,2</sup>, Zeqiang Ren<sup>1\*</sup> and Pengbo Zhang<sup>1\*</sup>

## Abstract

**Background** Circular RNAs (circRNAs) play important roles in the occurrence and development of cancer and chemoresistance. DNA damage repair contributes to the proliferation of cancer cells and resistance to chemotherapy-induced apoptosis. However, the role of circRNAs in the regulation of DNA damage repair needs clarification.

**Methods** RNA sequencing analysis was applied to identify the differentially expressed circRNAs. qRT-PCR was conducted to confirm the expression of hsa\_circ\_0007919, and CCK-8, FCM, single-cell gel electrophoresis and IF assays were used to analyze the proliferation, apoptosis and gemcitabine (GEM) resistance of pancreatic ductal adenocarcinoma (PDAC) cells. Xenograft model and IHC experiments were conducted to confirm the effects of hsa\_circ\_0007919 on tumor growth and DNA damage in vivo. RNA sequencing and GSEA were applied to confirm the downstream genes and pathways of hsa\_circ\_0007919. FISH and nuclear-cytoplasmic RNA fractionation experiments were conducted to identify the cellular localization of hsa\_circ\_0007919. ChIRP, RIP, Co-IP, ChIP, MS-PCR and luciferase reporter assays were conducted to confirm the interaction among hsa\_circ\_0007919, FOXA1, TET1 and the LIG1 promoter.

**Results** We identified a highly expressed circRNA, hsa\_circ\_0007919, in GEM-resistant PDAC tissues and cells. High expression of hsa\_circ\_0007919 correlates with poor overall survival (OS) and disease-free survival (DFS) of PDAC patients. Hsa\_circ\_0007919 inhibits the DNA damage, accumulation of DNA breaks and apoptosis induced by GEM in a LIG1-dependent manner to maintain cell survival. Mechanistically, hsa\_circ\_0007919 recruits FOXA1 and TET1 to

<sup>†</sup>Lei Xu, Xiao Ma and Xiuzhong Zhang contributed equally to this work.

\*Correspondence:  
Zeqiang Ren  
rzq0805@163.com  
Pengbo Zhang  
zpb\_ok@126.com

Full list of author information is available at the end of the article



© The Author(s) 2023. **Open Access** This article is licensed under a Creative Commons Attribution 4.0 International License, which permits use, sharing, adaptation, distribution and reproduction in any medium or format, as long as you give appropriate credit to the original author(s) and the source, provide a link to the Creative Commons licence, and indicate if changes were made. The images or other third party material in this article are included in the article's Creative Commons licence, unless indicated otherwise in a credit line to the material. If material is not included in the article's Creative Commons licence and your intended use is not permitted by statutory regulation or exceeds the permitted use, you will need to obtain permission directly from the copyright holder. To view a copy of this licence, visit <http://creativecommons.org/licenses/by/4.0/>. The Creative Commons Public Domain Dedication waiver (<http://creativecommons.org/publicdomain/zero/1.0/>) applies to the data made available in this article, unless otherwise stated in a credit line to the data.

decrease the methylation of the *LIG1* promoter and increase its transcription, further promoting base excision repair, mismatch repair and nucleotide excision repair. At last, we found that GEM enhanced the binding of QKI to the introns of *hsa\_circ\_0007919* pre-mRNA and the splicing and circularization of this pre-mRNA to generate *hsa\_circ\_0007919*.

**Conclusions** *Hsa\_circ\_0007919* promotes GEM resistance by enhancing DNA damage repair in a *LIG1*-dependent manner to maintain cell survival. Targeting *hsa\_circ\_0007919* and DNA damage repair pathways could be a therapeutic strategy for PDAC.

**Keywords** *hsa\_circ\_0007919*, *LIG1*, DNA damage repair, Pancreatic ductal adenocarcinoma, QKI

## Introduction

As one of the most aggressive and deadly malignancies, pancreatic ductal adenocarcinoma (PDAC) has become the fourth leading cause of cancer-related death and is expected to advance to the second leading cause of cancer-related death within decades [1, 2]. Despite the advances in the understanding of the molecular mechanisms and development of therapies for PDAC over the past few decades, its 5-year survival rate remains the lowest among all malignancies [3]. There is continuous proliferative signal transduction during the development of PDAC, such continuous proliferation induced by oncogene expression could cause DNA replication stress, resulting in genomic instability and even apoptosis [4]. Therefore, cancer cells respond to DNA damage via activation of DNA damage response (DDR) pathways, mainly including base excision repair, nucleotide excision repair, mismatch repair, homologous recombination and non-homologous terminal junction [5]. During the cell cycle, more than 6 million DNA base pairs are replicated, and this process can be affected by many sources of damage and replication stress [6]. DNA repair endows tumors with potent genomic stability and antiapoptotic ability, which can easily promote the malignant progression of tumors [7]. In addition, various chemotherapies for PDAC can cause specific types of DNA damage; for example, platinum alkylating agents and the topoisomerase inhibitor irinotecan can lead to DNA double-strand breaks (DSB), and the antimetabolic drugs 5-fluorouracil (5-FU) and gemcitabine (GEM) can cause single-base damage and single-strand DNA breaks (SSBs)[8], which can develop into DSBs upon accumulation [9]. To date, PARP inhibitors and cell cycle checkpoint inhibitors have proven to be effective therapies for PDAC [10]. Studies on DDR mechanism defects and inhibitors of DNA damage repair may provide new insights for the treatment of PDAC.

CircRNAs are a class of noncoding RNAs and are single-stranded, circular, closed RNAs widely present in eukaryotic cells [11]. CircRNAs are formed from pre-mRNAs of their host genes through selective back-splicing and circularization, and they have high stability and cannot be easily degraded by RNA enzymes [12]. CircRNAs have been found to be involved in multiple

steps of tumorigenesis and development, including DDR regulation [13]. CircSMARCA5 terminates SMARCA5 transcription at exon 15 to reduce its expression, thereby inhibiting SMARCA5-mediated DNA damage repair and cisplatin resistance in breast cancer (BC)[14]. CircITCH sponges miR-330-5p to increase SIRT6 expression, and SIRT6 then activates PARP1 to repair DNA damage to alleviate doxorubicin-induced cardiomyocyte damage and dysfunction [15]. However, there are few studies on the relationships between circRNAs and PDAC, and most of these have focused on miRNA-related research. Circ-MBOAT2 promotes the proliferation, metastasis and glutamine metabolism of PDAC cells through the miR-433-3p/GOT1 axis [16]. Cancer-associated fibroblast-specific circ-FARP1 binds to CAV1 and inhibits its ubiquitination by ZNRF1 to enhance the secretion of LIF; in addition, circ-FARP1 sponges miR-660-3p to increase the expression of LIF, thereby promoting the stemness and GEM resistance of PDAC cells [17]. To date, studies on the regulation of circRNAs on DNA damage in PDAC have not been reported.

In this study, we identified the highly expressed *hsa\_circ\_0007919* in GEM-resistant PDAC tissues and cells. *Hsa\_circ\_0007919* could inhibit the DNA damage and apoptosis induced by GEM chemotherapy and maintain cell survival. We found that mechanistically, *hsa\_circ\_0007919* recruits FOXA1 and TET1 to decrease the methylation of the *LIG1* promoter and enhance *LIG1* transcription, then *LIG1* involves in multiple DNA repair pathways to decrease GEM-related DNA damage. The function of *hsa\_circ\_0007919* was also verified in xenograft model in nude mice.

## Materials and methods

### Clinical tissue samples

A total of 95 pairs of PDAC tissues and adjacent tumor tissues were collected from Xuzhou Medical University Affiliated Hospital. Among them, 50 patients had not received radiotherapy or chemotherapy while 45 patients received GEM neoadjuvant therapy. This study was approved by Institutional Ethics Committee of Xuzhou Medical University Affiliated Hospital and informed consent were signed by all patients.

### Cell culture and transfection

The normal human pancreatic duct cell line hTERT-HPNE and PDAC cell lines PANC-1, CFPAC-1, BxPC-3 and MIA-PaCa2 were purchased from Chinese Academy of Science (Shanghai, China) cultured RPMI 1640 medium (Hyclone, USA) containing 10% Fetal Bovine Serum (FBS) (Gibco, USA), 100u/ml penicillin and 100 µg/ml streptomycin (Beyotime, China) in a cell incubator at 37°C with 5% CO<sub>2</sub>. For the construction of GEM-resistant PDAC cell lines, PANC-1 and CFPAC-1 cells were cultured with GEM (MCE, USA) at increasing concentration gradients. For 5-AzaC treatment, CRC cells were treated with 5µM of 5-AzaC (MCE, USA) for 72 h. All small interfering RNA (siRNA) and full-length plasmid of hsa\_circ\_0007919, LIG1, FOXA1, TET1 and negative control were purchased from GenePharma (Suzhou, China) and transfected into cells using Lipofectamine 2000 reagent (Invitrogen, USA) according to the manufacturer's protocol. All sequences of siRNAs are shown as follows:

si-hsa\_circ\_0007919 # 1 :  
5'-GACAGAUCAGGUGGAAGCTT-3';

si-hsa\_circ\_0007919 # 2 :  
5'-ACAGAUCAGGUGGAAGCATT-3';

si-LIG1#1: 5'-AGAAGAUAGACAUCAUCAAG-3';

si-LIG1#2: 5'-CGUCAUUUCUUCAAUAAAUA-3';

si-FOXA1: 5'-GGAUGUUAGGAACUGUGAAGA-3';

si-TET1: 5'-CGAAGCUACUGCAAUCAACA-3';

si-Ctrl: 5'-UUCUCCGAACGUGUCACGUTT-3'.

### RNA extraction and quantitative real-time PCR (qRT-PCR)

Total RNA was extracted from tissues and cells by RNA isolater Total RNA Extraction Kit (Vazyme, China), cDNA was synthesized by HiScript II Q RT SuperMix for qPCR (Vazyme, China) and the expression was detected by ChamQ SYBR qPCR Master Mix (Vazyme, China). All the data were normalized to GAPDH/U6 and the data from tissues were quantified by 2<sup>-ΔCt</sup> method while others were quantified by 2<sup>-ΔΔCt</sup> method. All the primers were synthesized by GENEray (Shanghai, China) and the sequences are shown as follows:

hsa\_circ\_0007919 - F :  
5'-AGGTGGAAGCAGGGAAAG-3';

hsa\_circ\_0007919 - R :  
5'-TCATGGGCAGCAACAGG-3';

ABR-F: 5'-GGTGGATTCTTCGGCTAT-3';

ABR-R: 5'-CACTTGGGCTCCGCTGT-3';

LIG1-F: 5'-GCCCTGCTAAAGGCCAGAAG-3';

LIG1-R: 5'-CATGGGAGAGGTGTCAGAGAG-3';

FOXA1-F: GCAATACTCGCCTTACGGCT-3';

FOXA1-R: TACACACCTTGGTAGTACGCC-3';

TET1-F: CATCAGTCAAGACTTTAAGCCCT-3';

TET1-R: CGGGTGGTTTAGGTTCTGTTT-3';

LIG1 P1-F: GCTAAAACCTCCTCCCC-3';

LIG1 P1-R: CATGAAGCATGTGACCG-3';

GAPDH-F: 5'-GGAGCGAGATCCCTCCAAAAT-3';

GAPDH-R: 5'-GGCTGTTGTCATACTTCTCATGG-3';

U6-F: 5'-CTCGCTTCGGCAGCAC-3';

U6-R: 5'-AACGCTTACGAATTTGCGT-3'.

### Identification of hsa\_circ\_0007919

qPCR product amplified by hsa\_circ\_0007919 primer was validated by Sanger-seq (Sangon, China). Total gDNA was extracted by FastPure Cell/Tissue DNA Isolation Mini Kit (Vazyme, China) and qPCR products amplified from cDNA and gDNA were separated in 1% agarose gel. Total RNA was treated with RNase R (Epicentre, USA) at 37°C for 30 min and were detected by qRT-PCR just as described above.

### Half maximal inhibitory concentration (IC50) detection assay

A total of 12 groups of 4×10<sup>3</sup> PDAC cells were placed into 96-well plate separately, then cells were treated with GEM at concentration of 0, 0.1, 0.2, 0.4, 0.8, 1.6, 3.2, 6.4, 12.8, 25.6, 51.2 and 102.4µM for 48 h and then detected as CCK-8 assay described.

### CCK-8 assay

Cells after transfection or GEM treatment were collected and counted, then 4×10<sup>3</sup> cells were placed into 96-well plate and cultured in incubator at 37°C. 24, 48, 72 and 96 h after, cells were incubated with 100 µl serum-free medium and 10 µl CCK-8 solution (Glpbio, USA) at 37°C for 2 h and measured at 450 nm wavelength (SPARK, Switzerland).

### Apoptosis detection assay

Cells after transfection or GEM treatment were collected by EDTA-free trypsin solution (Beyotime, China), then cells were washed by PBS and incubate with Annexin V and PI solution for 10 min and detected by the flow cytometer (BD, USA) according to the manufacturer's protocol of Cell Apoptosis Detection Kit (Biosharp, China).

### Western blot assay

Total protein was extracted from cells by RIPA lysis solution (Beyotime, China) and quantified by BCA Protein Assay Kit (Beyotime, China), protein was separated in SDS-PAGE and transferred to PVDF membrane (Millipore, Germany). After blocking with 5% skim milk, the membrane was incubated with primary antibodies and secondary antibodies and detected with Super ECL Detection Reagent (Yeasen, China) using a luminescent imaging system (Tanon, China). All used antibodies are shown as follows: anti-caspase3 (19677-1-AP, Proteintech, USA), anti-caspase9 (10380-1-AP, Proteintech,

USA), anti-BCL2 (68103-1-Ig, Proteintech, USA), anti-GAPDH (60004-1-Ig, Proteintech, USA), HRP-goat anti-rabbit IgG (H+L) (BF03008, Biodragon, China), HRP-goat anti-mouse IgG (H+L) (BF03001, Biodragon, China), anti- $\gamma$ -H2AX (AP0687, Abclonal, China), CoraLite594-conjugated Goat Anti-Rabbit IgG (H+L) (SA00013-4, Proteintech, USA), anti-LIG1 (18051-1-AP, Proteintech, USA), anti-Ki67 (GB111499, Servicebio, China), anti-FOXA1 (GTX100308, GeneTex, USA), anti-TET1 (AB\_2793752, Active Motif, USA), anti-QKI (13169-1-AP, Proteintech, USA).

#### Single cell gel electrophoresis

0.8% normal melting point agarose (Vicmed, China) was placed on glass slide, then  $5 \times 10^3$  cells in 0.6% low melting point agarose (Biosharp, China) was placed above and electrophoreted in a horizontal electrophoresis tank after lysis, at last cells were stained with PI solution (Biosharp, China) and the picture was photographed by inverted fluorescence microscope (Olympus, Japan).

#### DNA ladder assay

Total DNA of cells after transfection was extracted by FastPure Cell/Tissue DNA Isolation Mini Kit (Vazyme, China). Briefly, cells were collected and treated by RNase Solution and Proteinase K at room temperature. Then cells were mixed with buffer GB and anhydrous ethanol, after abstersion with washing buffer, DNA was dissolved into elution buffer. At last, DNA was separated in 1% agarose gel and photographed using luminescent imaging system (Tanon, China).

#### Immunofluorescence (IF)

Cells were fixed by 4% paraformaldehyde (Vicmed, China) and blocked by 5% Bovine Serum Albumin (BSA) (Solarbio, China), then cells were incubated with primary antibody, fluorescent secondary antibody and DAPI (Bioss, China) and photographed by confocal laser microscope (ZEISS, Germany).

#### Stable inhibition cell lines construction and xenograft model

PANC-1 and CFPAC-1 GEM-resistant cells were infected by hsa\_circ\_0007919 inhibition lentivirus (GenePharma, China) or negative control lentivirus and selected by puromycin (Solarbio, China) for over 2 weeks, the efficiency of lentivirus was detected by qPCR.  $5 \times 10^6$  lentivirus-infected cells were injected into blank region of nude mice (Gempharmatech, China) and were treated with GEM (50 mg/kg, i.p.) every 4 days. After measuring volumes of tumors every 5 days, the mice were sacrificed and the tumors were harvested 25 days after injection. All sequences of shRNAs are shown as follows:

sh-hsa\_circ\_0007919: 5'-CACCGAG-G T G G A A G C A G G G A A A G T T C G A A A A A T T G A T C A A T G C C G A G G A -3';  
sh-Ctrl: 5'-CACCGTTCTCCGAACGTGTCAC-GTTTCGAAAAACGTG ACACGTTCCGAGAA-3'

#### Immunohistochemical (IHC)

Tumors were fixed by 4% paraformaldehyde, paraffin embed and sliced into sections, sections were hydrated by xylene and gradient alcohol (Sinoreagent, China). Antigen of sections were repaired by citrate solution and blocked by goat serum, then sections incubated with primary and secondary antibodies according to the manufacturer's protocol of SP Kit (ZSGB-BIO, China) and stained by DAB Staining Kit (ZSGB-BIO, China) and hematoxylin solutions (Sinoreagent, China). The pictures of sections were photographed by inverted microscope (Olympus, Japan). Relative staining score was calculated using an IHC score analysis method according to the proportion of positively stained cells and the intensity of staining. The proportion of positive cells was scored as follows: 0 (0–5%), 1 (6–25%), 2 (26–50%), 3 (51–75%), 4 (>75%) and the intensity was scored as follows: 0 (negative), 1 (weak), 2 (moderate), 3 (strong).

#### TUNEL assay

The TUNEL assay was performed according to the manufacturer's protocol of TUNEL Apoptosis Detection Kit (Color Development) (Beyotime, China). Tissue sections was hydrated as described in IHC, after treated with Proteinase K at 37°C, the tissues were incubated with 3% hydrogen peroxide solution and biotin labeling solution containing TdT enzyme and biotin-dUDP away from light at 37°C, then the tissues were stained using Streptavidin-HRP solution and DAB staining solution and photographed by inverted microscope (Olympus, Japan).

#### Gene set enrichment analysis (GSEA)

GSEA was performed on the normalized data using the GSEA v2.0 tool (<http://www.broad.mit.edu/gsea/>). We compared the expression of genes in PANC-1 GEM-resistant cells transfected with hsa\_circ\_0007919 siRNA or negative control siRNA. Three gene sets were used for analysis (KEGG\_BASE\_EXCISION\_REPAIR, KEGG\_MISMATCH\_REPAIR, KEGG\_NUCLEOTIDE\_EXCISION\_REPAIR), and the detailed genes in the gene sets can be found in MSigDB (<http://software.broadinstitute.org/gsea/msigdb/genesets.jsp>). The P values of the differences between the two gene sets were analyzed with the Kolmogorov–Smirnov test.

#### Fluorescence in situ hybridization (FISH)

Cells were fixed by 4% paraformaldehyde and incubated with hybridization solution containing probes at 37°C

overnight, then cells were washed by SSC solution and stained with DAPI according to the manufacturer's protocol of FISH Kit (RIBOBIO, China). The images were photographed by confocal laser microscope (ZEISS, Germany).

#### Nuclear-cytoplasmic fractionation assay

Nuclear and cytoplasmic RNA was extracted by Cytoplasmic & Nuclear RNA Purification Kit (Norgen Biotek, Canada) according to the manufacturer's protocol, then the expression of hsa\_circ\_0007919 in nucleus and cytoplasm was detected by qPCR.

#### Chromatin isolation by RNA purification (ChIRP)

ChIRP was used to detect the protein binding with hsa\_circ\_0007919 and performed according to the manufacturer's protocol of ChIRP kit (Bersinbio, China). Briefly, cells were cross-linked with paraformaldehyde and lysed through sonication, and then the lysis solution was incubated with biotin-labeled hsa\_circ\_0007919 probes (RIBOBIO, China) and magnetic beads, ultimately the protein was extracted and detected by WB.

#### Co-immunoprecipitation (Co-IP)

Total protein extracted by cell lysis buffer for IP (Beyotime, China) was incubated with antibodies and magnetic beads, binding proteins were extracted by 2×SDS-PAGE Sample Loading Buffer (Beyotime, China) and detected by WB.

#### RNA binding protein immunoprecipitation (RIP)

RIP assay was conducted according to the manufacturer's protocol of RNA Immunoprecipitation Kit (GENESEED, China), mixture of RNA and protein was collected and incubated with antibodies and magnetic beads, RNA was extracted by adsorption column and detected by qPCR.

#### Chromatin immunoprecipitation (ChIP)

ChIP assay was conducted according to the manufacturer's protocol of Simple ChIP Enzymatic Chromatin IP Kit (CST, USA). Cells were mixed by 1% paraformaldehyde and chromatin was digested into fragments by enzymes. Then the solution was incubated with antibodies and magnetic beads and DNA was extracted from beads by purified centrifugal column, the binding DNA fragments were detected by qPCR.

#### Methylation-specific PCR (MS-PCR)

Total DNA was extracted by FastPure Cell/Tissue DNA Isolation Mini Kit (Vazyme, China), then DNA was denatured and bisulfite converted by EZ DNA Methylation-Gold Kit (ZYMO RESEARCH, USA) and amplified by Methylation Specific PCR Kit (TIANGEN, China) according to the manufacturer's protocol, the DNA was

ultimately separated in 1% agarose gel and photographed by luminescent imaging system. Methylated primer and unmethylated primer located in LIG1 promoter were generated by MethPrimer 2.0 (<http://www.urogene.org/methprimer2/>) and the sequences are shown as follows:

LIG1 M-F: 5'-GAGAAGAAGGTTTCGTTTTCGTAG-3';  
LIG1 M-R: 5'-ATAAAATAAATAAAATACCCC-GAAT-3';  
LIG1 U-F: 5'-GAGAAGAAGGTTTGTTTTGTG-3';  
LIG1 U-R: 5'-AAAATAAATAAATAAATAAATACCCCAAAT-3'.

#### Luciferase reporter assay

Luciferase reporter assay was conducted according to the manufacturer's protocol of Dual Luciferase Reporter Gene Assay Kit (Beyotime, China). Cells transfected with pGL3-basic plasmid containing LIG1 promoter (Genecreate, China) and pRL-TK control plasmid with or without hsa\_circ\_0007919 inhibition were collected for lysis, then the firefly luciferase detection reagent and renilla luciferase detection reagent was added into the solution and measured by Multifunctional microplate reader (SPARK, Switzerland) separately.

#### Statistical analysis

All values are expressed as mean±standard deviation (SD). The significance of the differences was measured by Student's t-test or one-way ANOVA. Kaplan–Meier analysis was used for survival analysis, and the differences of survival probabilities were measured by the log-rank test. The correlations between the expression of hsa\_circ\_0007919 and various clinicopathological variables were analyzed by Chi-Squared test.  $p < 0.05$  was considered significant. Statistical analyses were performed using SPSS version 25.0 (SPSS, Inc., USA).

## Results

### hsa\_circ\_0007919 is upregulated in GEM-resistant PDAC and predicts poor prognosis

We performed next-generation sequencing to identify circRNAs that contribute to GEM resistance in three GEM-resistant PDAC tissues and three GEM-sensitive PDAC tissues. A total of 62 circRNAs were differentially expressed ( $FC < -1$  or  $> 1$  and  $p < 0.05$ ), and hsa\_circ\_0007919 was significantly upregulated in GEM-resistant PDAC tissues compared with GEM-sensitive tissues ( $\log_2FC = 4.213454$ ,  $p = 0.000312$ , Fig. 1A). Then, we measured the expression of hsa\_circ\_0007919 in 50 pairs of non-GEM-resistant PDAC tissues and adjacent tissues and 45 pairs of GEM-resistant PDAC tissues and related adjacent tissues. The results showed that the expression of hsa\_circ\_0007919 was markedly upregulated in GEM-resistant PDAC tissues compared with GEM-sensitive PDAC tissues (Fig. 1B). Compared with

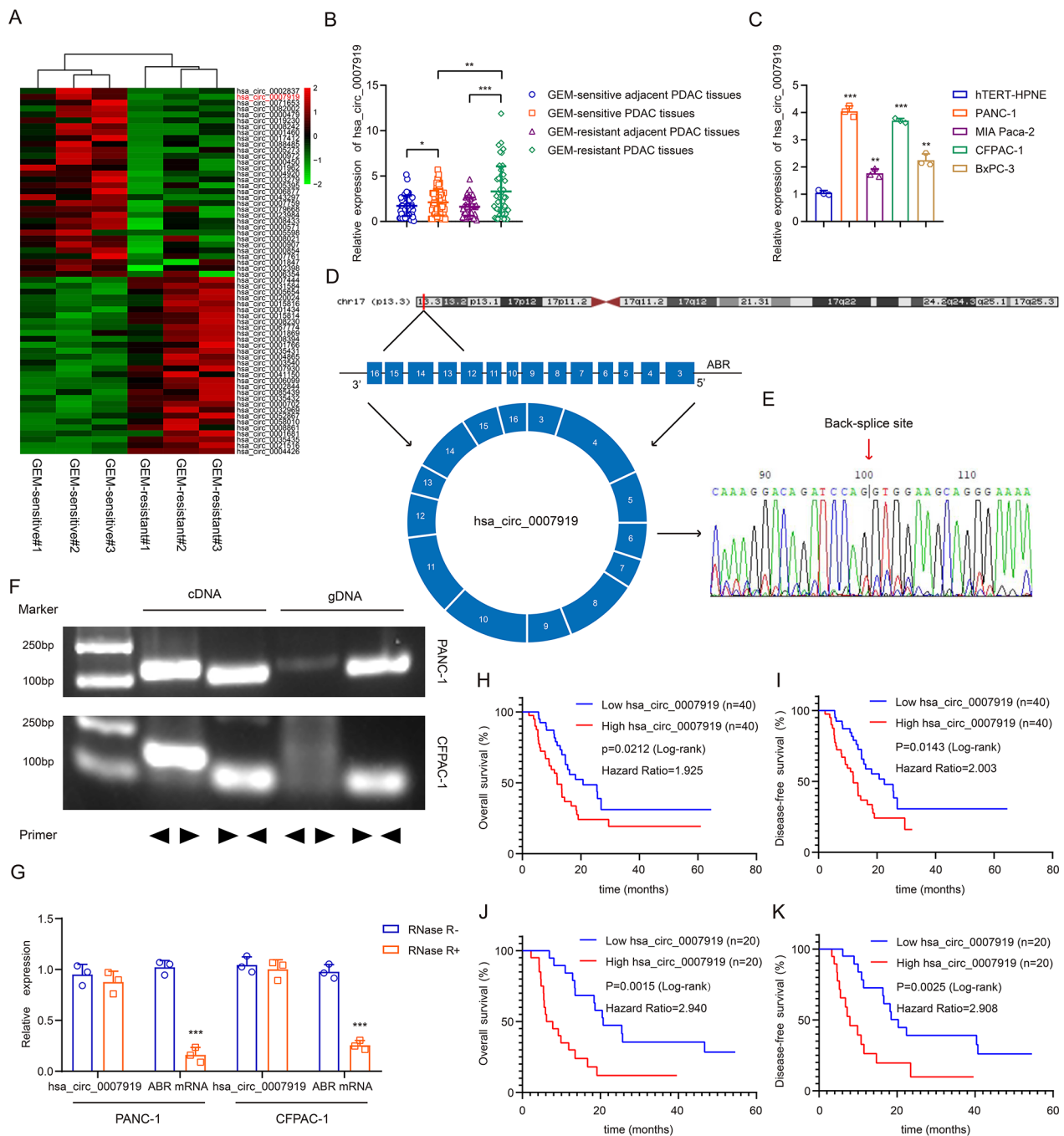


**Fig. 1** hsa\_circ\_0007919 is upregulated in GEM-resistant PDAC and predicts poor prognosis **(A)** Hierarchical clustering showing differentially expressed circRNAs in GEM-sensitive and GEM-resistant PDAC tissues ( $FC > 1$  or  $< -1$ ,  $p < 0.05$ ). **(B)** The relative expression of hsa\_circ\_0007919 in GEM-sensitive and GEM-resistant PDAC tissues and corresponding adjacent PDAC tissues. **(C)** The relative expression of hsa\_circ\_0007919 in PDAC cells and normal pancreatic cells. **(D)** The genomic location and back-splicing of hsa\_circ\_0007919. **(E)** The splicing site of hsa\_circ\_0007919 validated by Sanger-seq. **(F)** PCR and agarose gel electrophoresis analysis of the presence of hsa\_circ\_0007919 and ABR in cDNA and gDNA samples from PDAC cells. **(G)** Expression of hsa\_circ\_0007919 and ABR in PDAC cells with or without RNase R treatment. **(H-I)** Kaplan-Meier analysis of the OS rate and DFS rate in PDAC patients with high or low expression of hsa\_circ\_0007919. **(J-K)** Kaplan-Meier analysis of the OS rate and DFS rate in GEM-resistant PDAC patients with high or low expression of hsa\_circ\_0007919. Data are the means  $\pm$  SDs ( $n = 3$  independent experiments), \*  $p < 0.05$ , \*\*  $p < 0.01$ , \*\*\*  $p < 0.001$

that in normal human pancreatic duct cells, the expression of hsa\_circ\_0007919 was increased in PDAC cells, including PANC-1, CFPAC-1, BxPC-3 and MIA-Paca2, and its expression level was relatively high in PANC-1 and CFPAC-1 cells (Fig. 1C). We next evaluated the structure of hsa\_circ\_0007919, which is derived from exons 3–16 of the ABR gene, and validated the circularization site of hsa\_circ\_0007919 by Sanger-seq (Fig. 1D-E); the results were consistent with the data obtained from the circBase database (<https://www.circbase.org>). We also designed divergent and convergent primers to detect the expression of hsa\_circ\_0007919 in both cDNA and gDNA. The

**Table 1** Relationships between hsa\_circ\_0007919 expression and the clinicopathological characteristics of PDAC patients

Clinicopathological parameters	Cases	hsa_circ_0007919 level		$\chi^2$	p-value
		High(40)	Low(40)		
Age <sup>a</sup>	80			0.220	0.639
< 60	28	13	15		
≥ 60	52	27	25		
Gender <sup>a</sup>				0.549	0.459
Female	23	13	10		
Male	57	27	30		
Tumor location <sup>a</sup>				0.879	0.348
Head	52	28	24		
Body and tail	28	12	16		
Vascular invasion <sup>a</sup>				4.588	<b>0.032*</b>
Yes	62	35	27		
No	18	5	13		
Nerve invasion <sup>a</sup>				4.267	<b>0.039*</b>
Yes	60	34	26		
No	20	6	14		
Degree of differentiation <sup>b</sup>				2.453	0.313
Highly	2	0	2		
Moderately	27	12	15		
Poorly	51	28	23		
T stage <sup>b</sup>				9.895	<b>0.018*</b>
T1	9	1	8		
T2	33	14	19		
T3	20	13	7		
T4	18	12	6		
Lymph node metastasis <sup>b</sup>				7.296	<b>0.034*</b>
N0	36	12	24		
N1	34	22	12		
N2	10	6	4		
TNM stage <sup>a</sup>				11.958	<b>0.003**</b>
I	24	5	19		
II	32	19	13		
III	24	16	8		

<sup>a</sup> Pearson chi-square test; <sup>b</sup> Fisher's exact test. \* $P < 0.05$ , \*\* $P < 0.01$

TNM staging is classified according to the 8th edition of the American Joint Committee on Cancer (AJCC).

results showed that hsa\_circ\_0007919 could be amplified from cDNA but not gDNA (Fig. 1F), and the resistance of hsa\_circ\_0007919 to digestion by the RNase R exonuclease confirmed that it was indeed circular (Fig. 1G). At last, we explored data from clinical tissue samples to analyze the correlations between hsa\_circ\_0007919 expression and clinicopathological features. We divided the 80 PDAC patients with or without GEM treatment into two groups with high expression (40 samples) or low expression (40 samples) of hsa\_circ\_0007919. As shown in Table 1, high expression of hsa\_circ\_0007919 was significantly correlated with vascular invasion ( $p = 0.032$ ), nerve invasion ( $p = 0.039$ ), T stage ( $p = 0.018$ ), lymph node metastasis ( $p = 0.034$ ) and TNM stage ( $p = 0.003$ ), while there was no prominent association of hsa\_circ\_0007919 expression with age, gender, tumor location, degree of differentiation. Moreover, analysis of the relationship of hsa\_circ\_0007919 expression with overall survival (OS) and disease-free survival (DFS) of GEM-resistant patients showed that high expression of hsa\_circ\_0007919 predicted poor OS and DFS ( $p < 0.05$ ) (Fig. 1H-I). Furthermore, we divided the 40 GEM-treated PDAC patients into two groups with high expression ( $n = 20$ ) or low expression ( $n = 20$ ) of hsa\_circ\_0007919 and found that high expression of hsa\_circ\_0007919 similarly predicted poor OS and DFS ( $p < 0.01$ ) (Fig. 1J-K).

### hsa\_circ\_0007919 inhibits DNA damage and gemcitabine sensitivity

GEM is one of the common chemotherapy drugs in the clinical treatment of PDAC and can cause SSBs and DSBs by mediating base damage; however, PDAC patients often have adverse clinical outcomes due to chemoresistance [18]. Since hsa\_circ\_0007919 was upregulated in GEM-resistant PDAC tissues, we investigated its function in GEM-resistant cells. Firstly, we silenced hsa\_circ\_0007919 in PDAC cells and found that hsa\_circ\_0007919 inhibition increased GEM sensitivity (Fig. 2A-B, S1A). Then, we constructed GEM-resistant PDAC cell lines, PANC-1/GEM and CFPAC-1/GEM (Fig. 2C-D), and found that hsa\_circ\_0007919 was highly expressed in these GEM-resistant cells (Fig. 2E). Once again, we silenced hsa\_circ\_0007919 in both of these GEM-resistant cell lines and overexpressed it in normal PANC-1 and CFPAC-1 cells treated with GEM (Fig. S1B-C), and the results of the CCK-8 assay, FCM assay and DNA Ladder assay indicated that hsa\_circ\_0007919 silencing decreased the proliferation and increased the apoptosis of cells, while hsa\_circ\_0007919 overexpression had the opposite effects (Fig. 2F-K, S1D-G). Consistent with the apoptosis assay results, hsa\_circ\_0007919 silencing increased the levels of cleaved caspase 3 and cleaved caspase 9 and decreased BCL2 expression, while hsa\_circ\_0007919 overexpression decreased the levels of

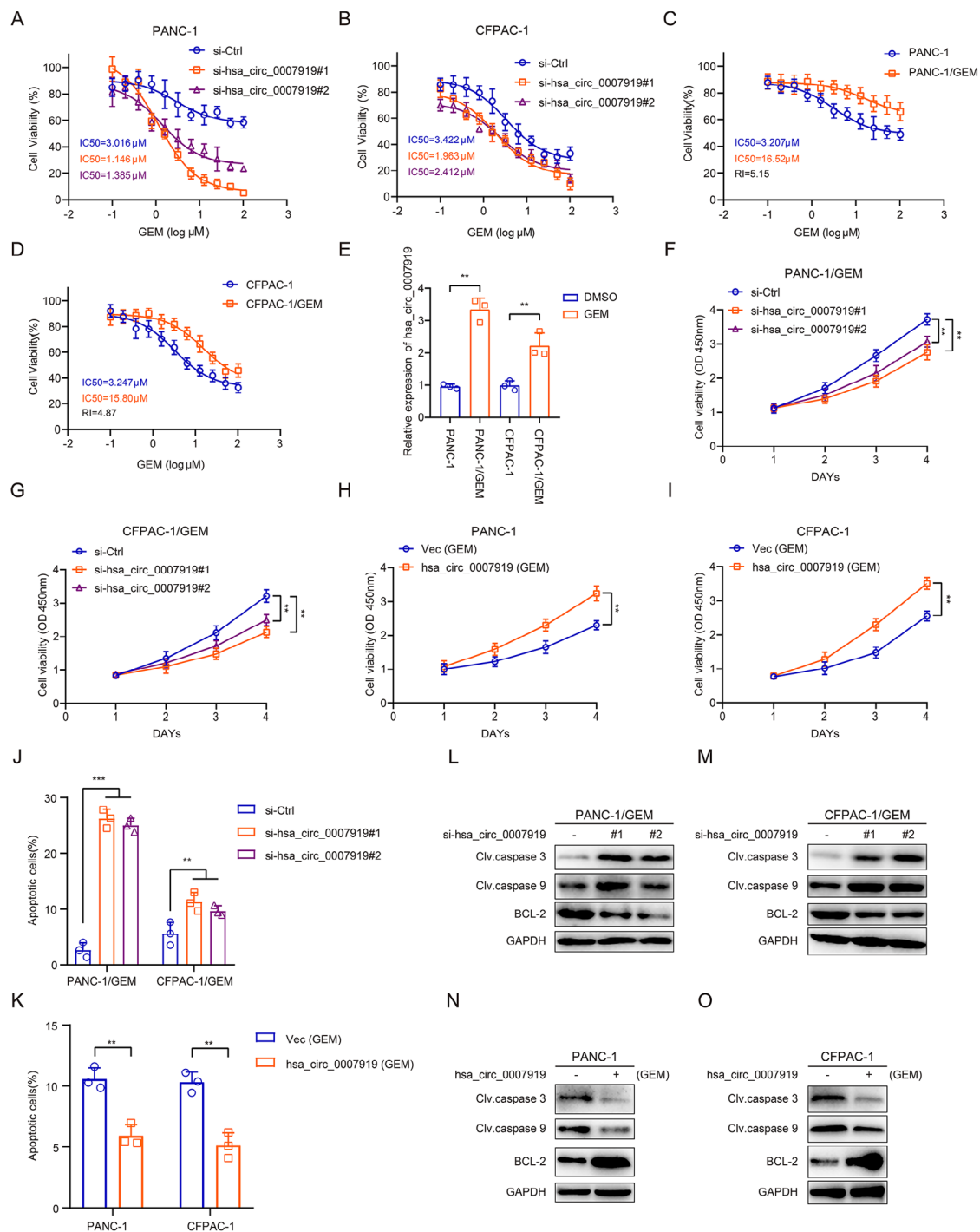


**Fig. 2** hsa\_circ\_0007919 inhibits gemcitabine sensitivity and apoptosis of GEM-resistant PDAC cells **(A-B)** CCK-8 analysis of the sensitivity of PDAC cells with or without hsa\_circ\_0007919 inhibition under different concentrations of GEM. **(C-D)** CCK-8 analysis of the sensitivity of normal and GEM-resistant PDAC cells under different concentrations of GEM. **(E)** Expression of hsa\_circ\_0007919 in normal and PDAC-resistant PDAC cells. **(F-G)** CCK-8 analysis of the proliferation of GEM-resistant PDAC cells with or without hsa\_circ\_0007919 inhibition. **(H-I)** CCK-8 analysis of the proliferation of PDAC cells with or without hsa\_circ\_0007919 overexpression under GEM treatment condition. **(J)** Flow cytometry analysis of the apoptotic rate of PDAC-resistant PDAC cells with or without hsa\_circ\_0007919 inhibition. **(K)** Flow cytometry analysis of the apoptotic rate of PDAC PDAC cells with or without hsa\_circ\_0007919 overexpression under GEM treatment condition. **(L-M)** Expression of apoptosis-related proteins in GEM-resistant PDAC cells with or without hsa\_circ\_0007919 inhibition. **(N-O)** Expression of apoptosis-related proteins in GEM PDAC cells with or without hsa\_circ\_0007919 overexpression under GEM treatment condition. Data are the means ± SDs (n=3 independent experiments), \*\*  $p < 0.01$ , \*\*\*  $p < 0.001$

cleaved caspase 3 and cleaved caspase 9 and increased BCL2 expression (Fig. 2L-O). GEM, which functions as a pyrimidine antimetabolic agent, can induce single-base damage and lead to DNA breaks, so we evaluated the influence of hsa\_circ\_0007919 on DNA damage and found that hsa\_circ\_0007919 silencing increased the tail of single cells in gel electrophoresis and the accumulation of  $\gamma$ -H2AX in the nucleus, while hsa\_circ\_0007919 overexpression decreased these parameters (Fig. 3A-B). At last, we established xenograft model in nude mice and found that the volume and weight of tumors formed by hsa\_circ\_0007919-silenced PANC-1/GEM and PANC-1/GEM cells were decreased compared with those of tumors formed by control cells (Fig. 3C-G). The IHC, TUNEL assay and qPCR results showed that hsa\_circ\_0007919 silencing decreased the expression of Ki-67 and increased the expression of caspase3 and  $\gamma$ -H2AX and cell apoptosis (Fig. 3H-J, S2A-B). These results revealed that hsa\_circ\_0007919 enhances GEM resistance in PDAC cells by decreasing DNA damage to promote proliferation and reduce apoptosis.

#### **hsa\_circ\_0007919 inhibits DNA damage through LIG1-mediated repair pathways**

To confirm how hsa\_circ\_0007919 inhibits DNA damage and influences GEM sensitivity, we performed RNA-seq to identify the differentially expressed genes in hsa\_circ\_0007919-silenced PANC-1/GEM cells compared with control cells. There were 520 upregulated and 219 downregulated genes (Fig. 4A), and KEGG analysis and GSEA showed that these genes were enriched in multiple DNA damage repair pathways, including base excision repair, mismatch repair and nucleotide excision repair (Fig. 4B-E). LIG1 was the most significantly downregulated gene common to all of these pathways (Fig. 4E, S2C-E). LIG1, a member of the DNA ligase family, has been reported to play an important role in DNA recombination in almost all DNA damage repair pathways [19]. Therefore, we measured the expression of LIG1 and found that it was also highly expressed in GEM-resistant PDAC tissues compared with normal PDAC tissues and was positively correlated with the expression of hsa\_circ\_0007919 in PDAC tissues (Fig. 4G-I). The mRNA and protein expression levels of LIG1 were decreased after hsa\_circ\_0007919 silencing and increased when hsa\_circ\_0007919 was overexpressed (Fig. 4J-M). These results revealed that hsa\_circ\_0007919 induces LIG1 expression to activate DNA damage repair pathways and enhance resistance to GEM in PDAC cells.

#### **LIG1 reversed the effects of hsa\_circ\_0007919 on cell proliferation, apoptosis and DNA damage**

To confirm that LIG1 is the downstream target of hsa\_circ\_0007919, we investigated the role of LIG1 in

GEM-resistant PDAC cells and found that silencing LIG1 resulted in decreased proliferation and increased apoptosis and DNA damage (Fig. 5A-G, S3A-B). Moreover, we further overexpressed LIG1 in PANC-1/GEM and PANC-1/GEM cells with stable hsa\_circ\_0007919 silencing (Fig. S3C-D) and found that LIG1 overexpression reversed cell proliferation, apoptosis and DNA damage affected by hsa\_circ\_0007919 silencing (Fig. 5H-N, S3E). These results revealed that hsa\_circ\_0007919 increases LIG1 expression to promote cell proliferation and reduce apoptosis and DNA damage.

#### **hsa\_circ\_0007919 binds to FOXA1 and TET1 to promote LIG1 transcription**

To investigate how hsa\_circ\_0007919 increases the expression of LIG1, we performed FISH and nuclear-cytoplasmic RNA fractionation assays, and the results showed that hsa\_circ\_0007919 was mainly distributed in the nucleus (Fig. 6A-B). We determined the overlap between the proteins that bind to hsa\_circ\_0007919 and the proteins that bind to LIG1 mRNA using the circAtlas 2.0 (<http://circatlas.biols.ac.cn/>) and ENCORI (<http://starbase.sysu.edu.cn/>) databases but could not identify any overlapping proteins (Fig. S4A). Then, we determined the overlap between the proteins that bind to hsa\_circ\_0007919 and those that bind to the promoter of LIG1 using the circAtlas 2.0 and SPP (<https://www.signalingpathways.org>) databases, and FOXA1 was identified as the protein with the most significant overlap (Fig. 6C). We further predicted that there may be other proteins that function together with FOXA1 and identified TET1, which binds to FOXA1, using the STRING database (<https://cn.string-db.org/>) (Fig. 6D). Since FOXA1 functions as a transcriptional promoter in multiple kinds of cancers and TET1 functions as a DNA methylhydroxylase to decrease the methylation level of various gene promoters and enhance their transcription [20, 21], we predicted that hsa\_circ\_0007919 binds to FOXA1 and TET1 to promote the transcription of LIG1. We first silenced FOXA1 and TET1 and found that the expression of LIG1 was decreased (Fig. 6E-H, S4B-C), and the results of the co-IP assay confirmed the interaction between FOXA1 and TET1 in GEM-resistant cells (Fig. 6I-J). At the same time, we silenced TET1 in FOXA1-silenced GEM-resistant cells and found that TET1 could enhanced the inhibition ability of FOXA1-silencing on LIG1, while overexpressing TET1 could partly reverse the inhibition ability of FOXA1-silencing on LIG1, which indicated that FOXA1 and TET1 play the synergistic effect in the regulation of LIG1 (Fig. 6K-L). Then, we performed a ChIRP assay and found that hsa\_circ\_0007919 could bind to FOXA1 and TET1 (Fig. 6M-N). Furthermore, we used a RIP assay to confirm that FOXA1 and TET1 can interact with hsa\_circ\_0007919,

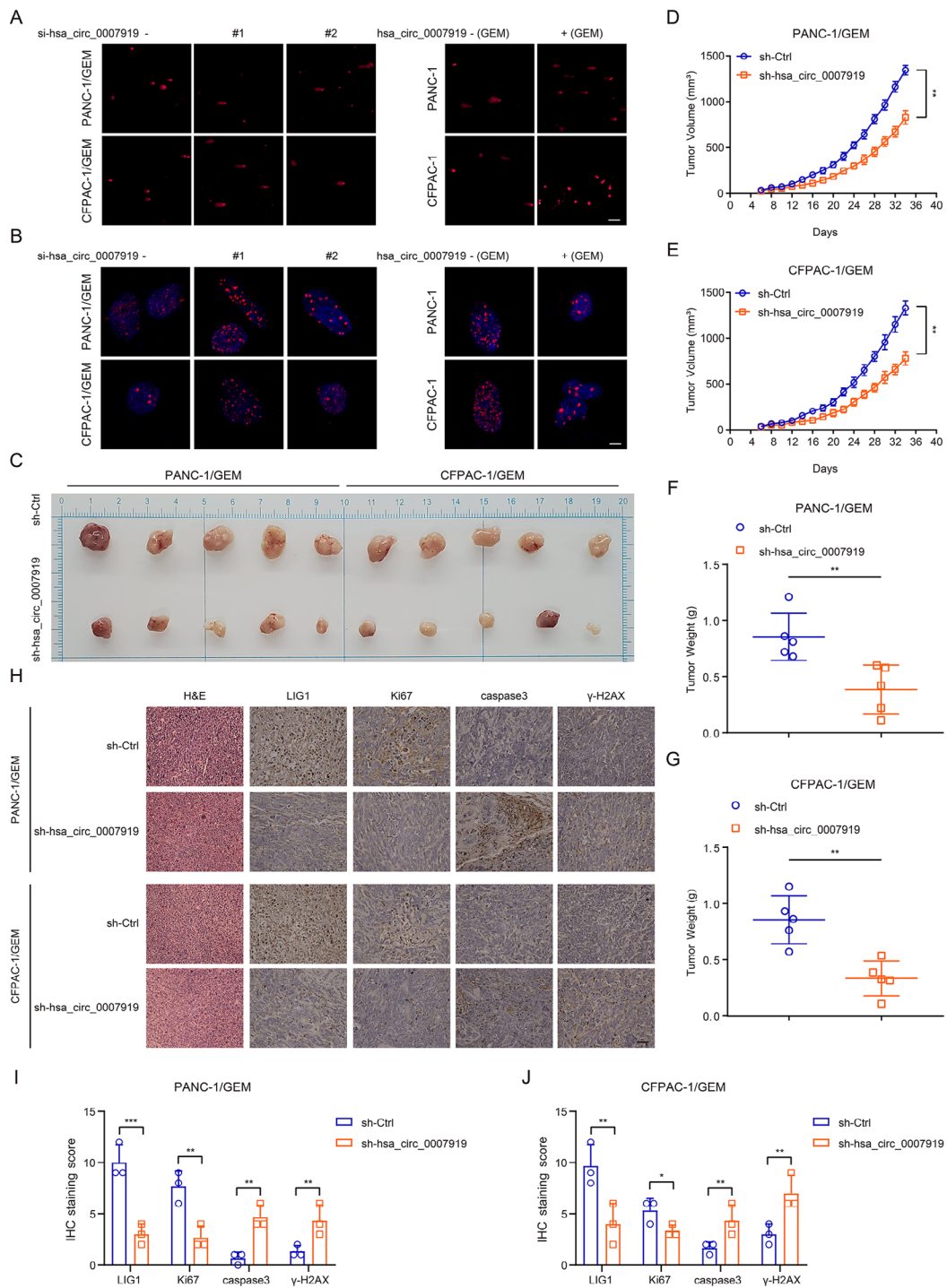


**Fig. 3** hsa\_circ\_0007919 inhibits DNA damage of GEM-resistant PDAC cells and proliferation of tumor in vivo **(A)** Comet analysis of the DNA damage of GEM-resistant PDAC cells with or without hsa\_circ\_0007919 inhibition and of the DNA damage of PDAC cells with or without hsa\_circ\_0007919 overexpression under GEM treatment condition (200×). **(B)** IF analysis of γ-H2AX accumulation in GEM-resistant PDAC cells with or without hsa\_circ\_0007919 inhibition and of γ-H2AX accumulation in PDAC cells with or without hsa\_circ\_0007919 overexpression under GEM treatment condition (1000×). **(C)** Image of tumors formed by GEM-resistant PDAC cells with or without hsa\_circ\_0007919 inhibition (n = 5). **(D-E)** Growth curves of tumors formed by GEM-resistant PDAC cells with or without hsa\_circ\_0007919 inhibition (n = 5). **(F-G)** Weights of tumors formed by GEM-resistant PDAC cells with or without hsa\_circ\_0007919 inhibition (n = 5). **(H)** IHC analysis of the expression of LIG1, Ki67, caspase 3 and γ-H2AX in tumors formed by GEM-resistant PDAC cells with or without hsa\_circ\_0007919 inhibition (400×). **(I-J)** IHC staining score analysis of images from Fig. 3H. Data are the means ± SDs (n = 3 independent experiments), \*\* p < 0.01

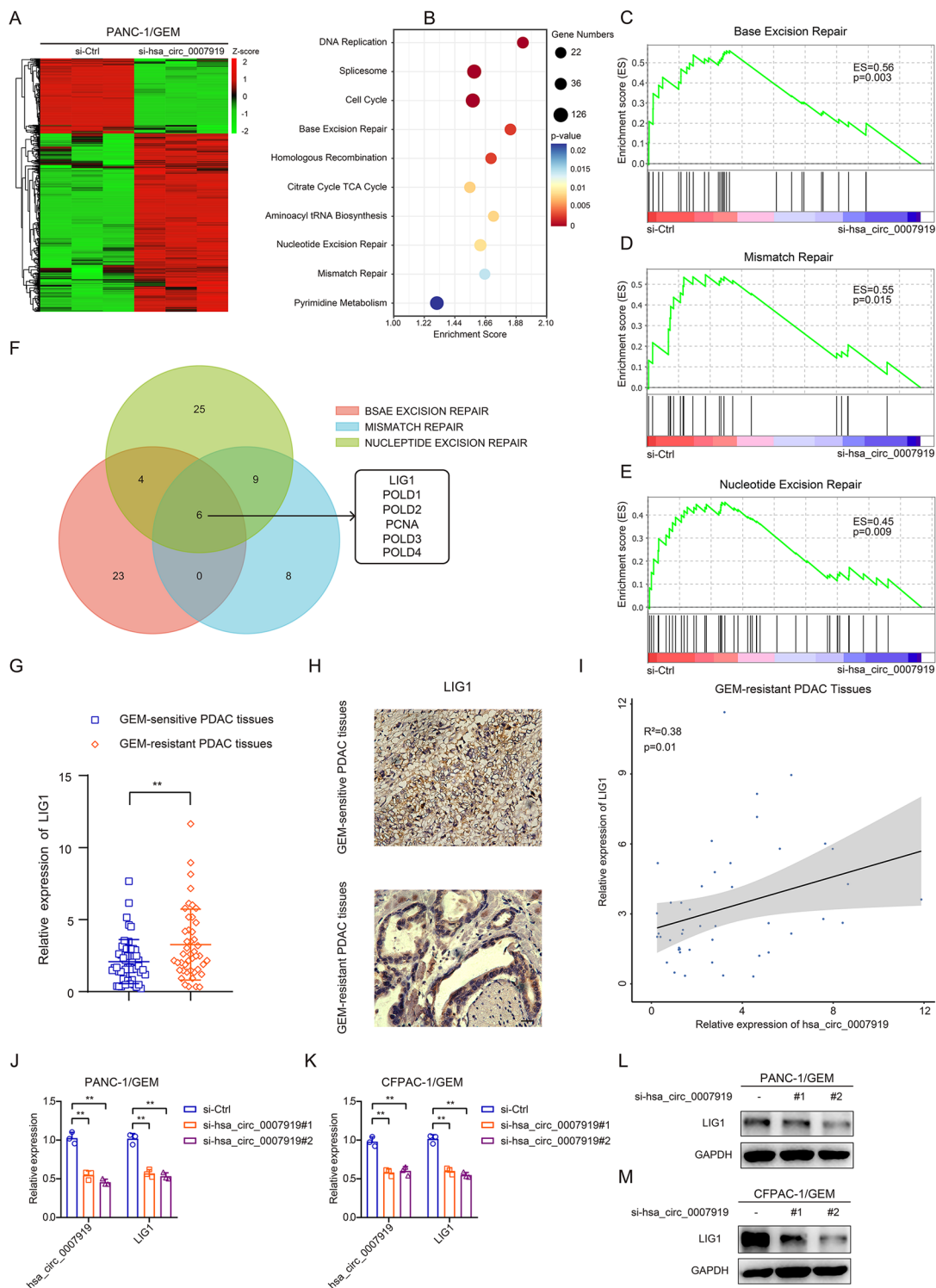


**Fig. 4** hsa\_circ\_0007919 inhibits DNA damage through LIG1-mediated repair pathways **(A)** Hierarchical clustering showing differentially expressed genes in GEM-resistant PDAC cells with or without hsa\_circ\_0007919 inhibition ( $FC > 1$  or  $< -1$ ,  $p < 0.05$ ). **(B)** KEGG enrichment analysis of hsa\_circ\_0007919-regulated gene expression events. **(C-E)** GSEA enrichment analysis of hsa\_circ\_0007919-regulated gene expression events. **(F)** Venn diagram showing overlapping genes between differentially expressed genes from base excision repair, mismatch repair and nucleotide excision repair pathways. **(G-H)** Expression of LIG1 in GEM-sensitive and -resistant PDAC tissues at mRNA and protein level (400 $\times$ ). **(I)** Correlation analysis of hsa\_circ\_0007919 and LIG1 expression in GEM-resistant tissues. **(J-M)** Expression of LIG1 in GEM-resistant cells with or without hsa\_circ\_0007919 inhibition at mRNA and protein level. Data are the means  $\pm$  SDs ( $n = 3$  independent experiments), **\*\***  $p < 0.01$

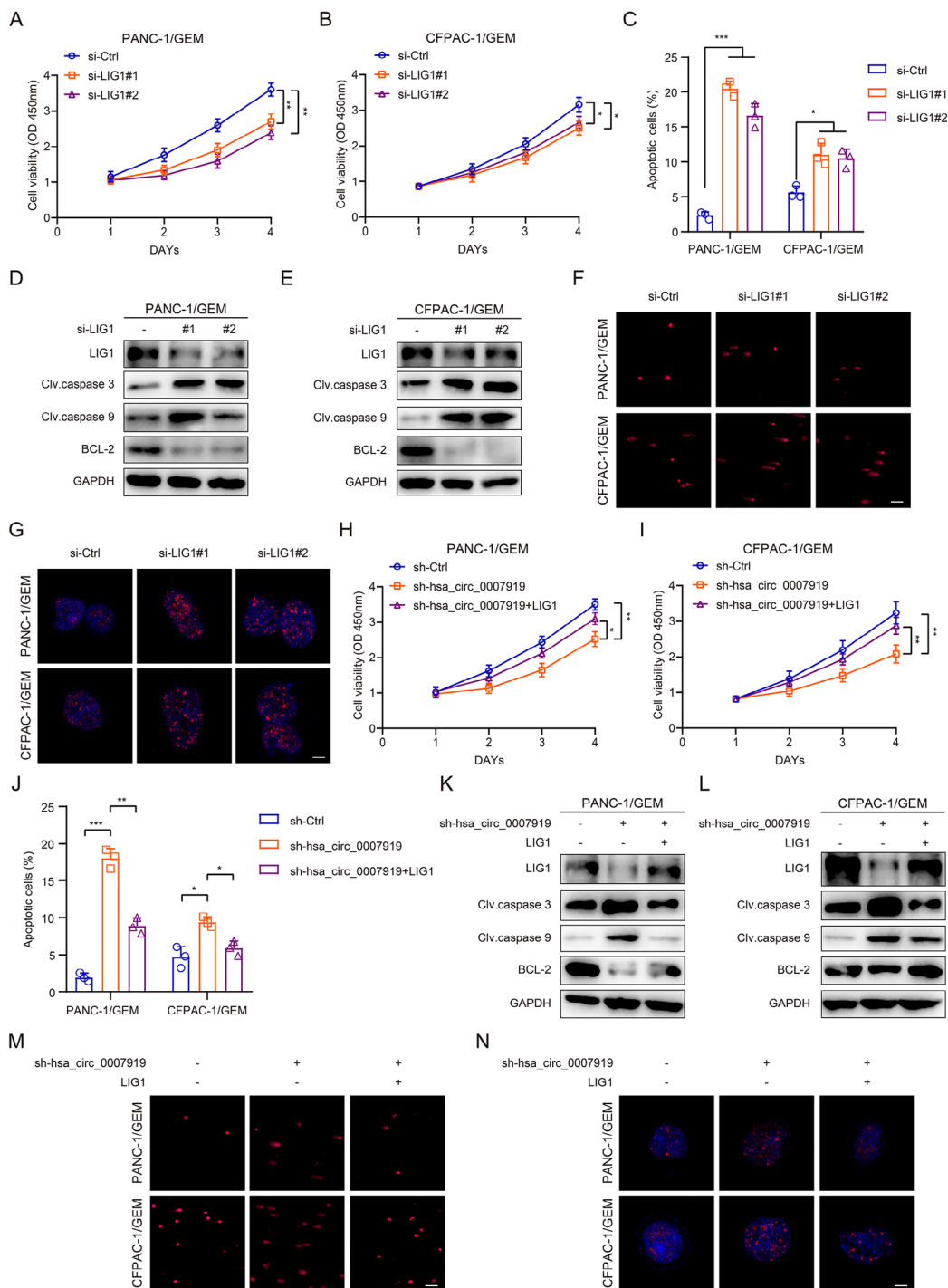


**Fig. 5** LIG1 reversed cell proliferation, apoptosis and DNA damage effects of hsa\_circ\_0007919 **(A-B)** CCK-8 analysis of the proliferation of GEM-resistant PDAC cells with or without LIG1 inhibition. **(C)** Flow cytometry analysis of the apoptotic rate of PDAC-resistant PDAC cells with or without LIG1 inhibition. **(D-E)** Expression of apoptosis-related proteins in GEM-resistant PDAC cells with or without LIG1 inhibition. **(F)** Comet analysis of the DNA damage of GEM-resistant PDAC cells with or without LIG1 inhibition (200×). **(G)** IF analysis of γ-H2AX accumulation in GEM-resistant PDAC cells with or without LIG1 inhibition (1000×). **(H-I)** CCK-8 analysis of the proliferation of hsa\_circ\_0007919-inhibited GEM-resistant PDAC cells with or without LIG1 overexpression. **(J)** Flow cytometry analysis of the apoptotic rate of hsa\_circ\_0007919-inhibited PDAC-resistant PDAC cells with or without LIG1 overexpression. **(K-L)** Expression of apoptosis-related proteins in hsa\_circ\_0007919-inhibited GEM-resistant PDAC cells with or without LIG1 overexpression. **(M)** Comet analysis of the DNA damage of hsa\_circ\_0007919-inhibited GEM-resistant PDAC cells with or without LIG1 overexpression (200×). **(N)** IF analysis of γ-H2AX accumulation in hsa\_circ\_0007919-inhibited GEM-resistant PDAC cells with or without LIG1 overexpression (1000×). Data are the means ± SDs (n = 3 independent experiments), \*  $p < 0.05$ , \*\*  $p < 0.01$ , \*\*\*  $p < 0.001$

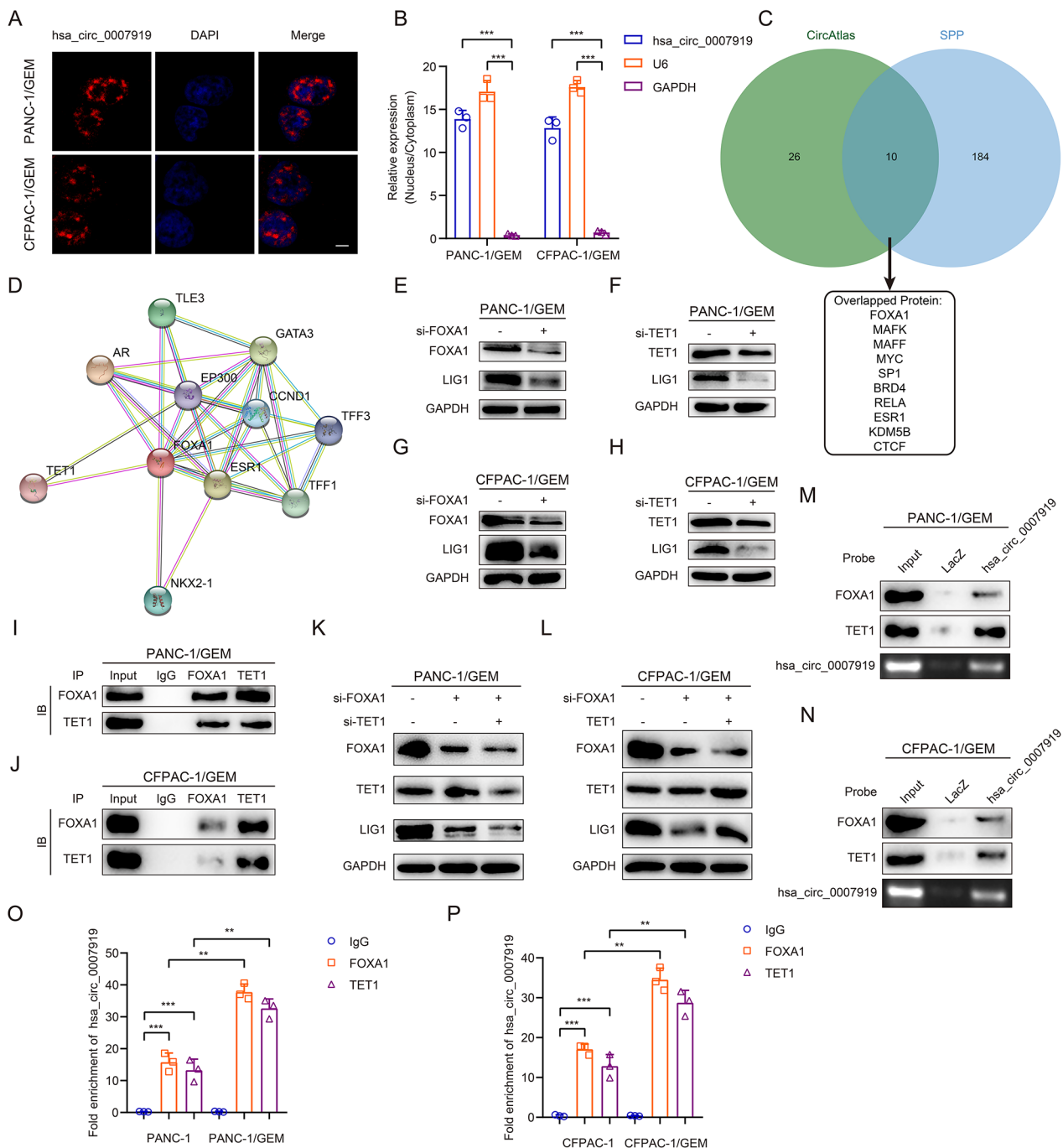


**Fig. 6** hsa\_circ\_0007919 binds FOXA1 and TET1 in GEM-resistant PDAC cells  
**(A)** FISH analysis of the cellular localization of hsa\_circ\_0007919. The hsa\_circ\_0007919 probes were red while nuclei were stained with DAPI (1000x).  
**(B)** Nuclear-cytoplasmic fractionation assay analysis of hsa\_circ\_0007919 location in GEM-resistant PDAC cells, the U6 and GAPDH were used as nuclear and cytoplasmic controls.  
**(C)** Venn diagram showing overlapped genes between interacting with hsa\_circ\_0007919 and interacting with LIG1 promoter region.  
**(D)** Protein-protein interaction network analysis of proteins interact with FOXA1.  
**(E-H)** Expression of LIG1 in GEM-resistant PDAC cells with or without FOXA1 or TET1 inhibition.  
**(I-J)** IP assay analysis of the interaction between FOXA1 and TET1 in GEM-resistant PDAC cells.  
**(K-L)** Expression of LIG1 in FOXA1-silenced GEM-resistant PDAC cells with TET1 inhibition or overexpression.  
**(M-N)** ChIRP assay analysis of the interaction between hsa\_circ\_0007919 and FOXA1 or TET1 in GEM-resistant PDAC cells.  
**(O-P)** RIP assay analysis of the interaction between FOXA1 or TET1 and hsa\_circ\_0007919 in normal or GEM-resistant PDAC cells. Data are the means  $\pm$  SDs (n = 3 independent experiments), \*\*  $p < 0.01$ , \*\*\*  $p < 0.001$

and this interaction was enhanced in GEM-resistant cells (Fig. 6O-P).

To investigate the interaction among FOXA1, TET1 and the LIG1 promoter, we analyzed the binding site between FOXA1 and the LIG1 promoter using the JASPAR database (<https://jaspar.genereg.net/>) and predicted the CpG islands in the LIG1 promoter using the MethPrimer 2.0 database (<http://www.urogene.org/methprimer2/>). Among the 6 sites identified by JASPAR and the 4 predicted CpG islands, we found that site 6 in the LIG1 promoter was the most enriched and thus chose the -1411 to -1273 region (P1) for further research

(Fig. 7A-B, S4D-E), and we found that treatment with 5-AzaC increased LIG1 expression in GEM-resistant cells (Fig. 7C). The results of the ChIP assay revealed that FOXA1 and TET1 bind to the LIG1 promoter region P1, and hsa\_circ\_0007919 inhibition decreased this binding capacity (Fig. 7D). The MS-PCR assay results showed that silencing hsa\_circ\_0007919 or TET1 increased the DNA methylation level in the LIG1 promoter (Fig. 7F), while overexpressing hsa\_circ\_0007919 or TET1 had the opposite effect (Fig. 7E and G). Furthermore, we performed a luciferase reporter assay and found that silencing hsa\_circ\_0007919, FOXA1 or TET1 decreased the

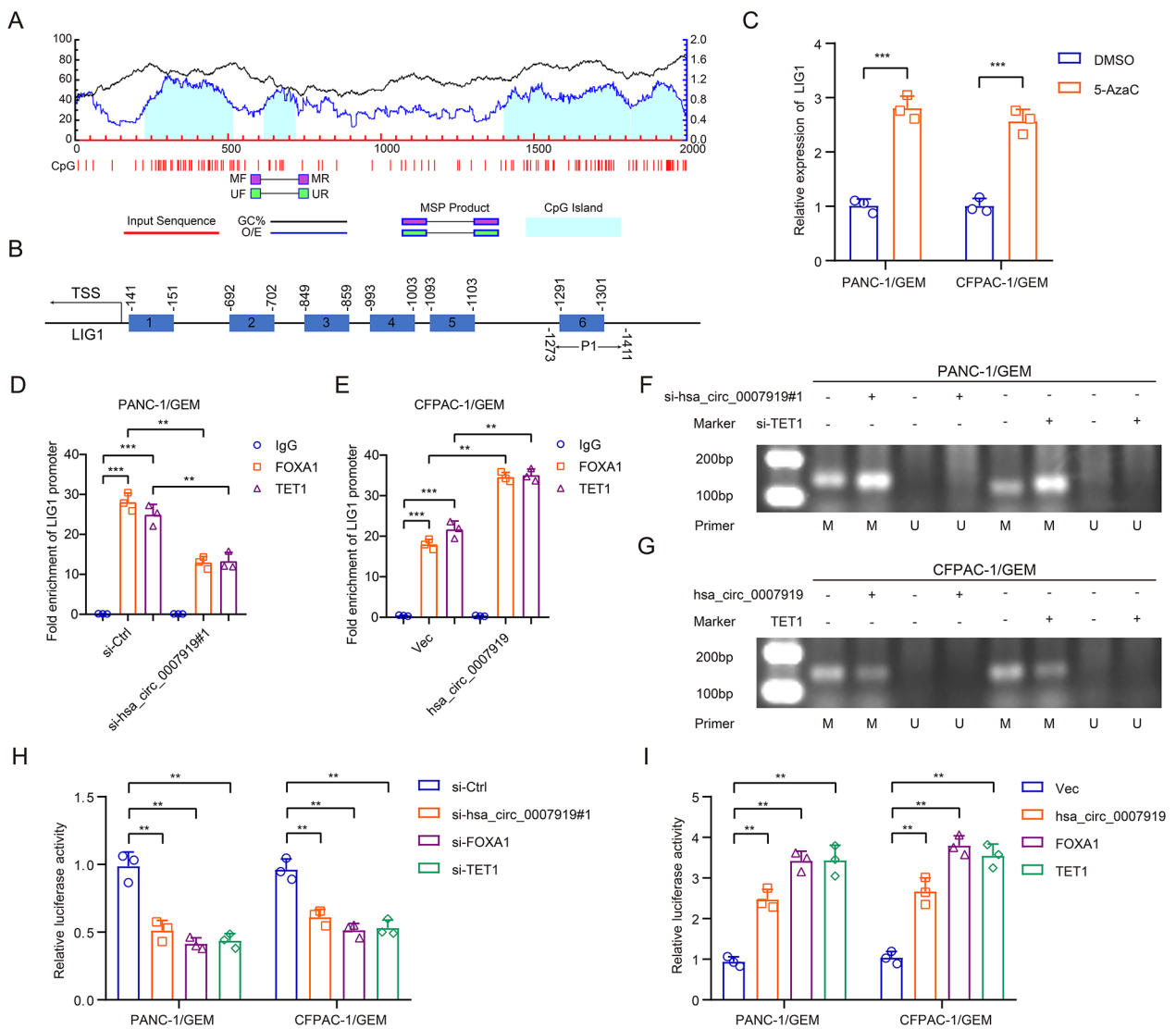


**Fig. 7** hsa\_circ\_0007919 recruits FOXA1 and TET1 to promote LIG1 transcription **(A)** DNA methylation analysis of CpG island of LIG1 promoter. **(B)** Interaction region predicted between FOXA1 and LIG1 promoter. **(C)** Expression of LIG1 in GEM-resistant PDAC cells with or without 5-AzaC treatment. **(D-E)** ChIP assay analysis of the interaction between FOXA1 or TET1 and LIG1 promoter. **(F-G)** MS-PCR analysis of methylation level of LIG1 promoter in GEM-resistant PDAC cells with or without hsa\_circ\_0007919 or TET1 inhibition and with or without hsa\_circ\_0007919 or TET1 overexpression. **(H-I)** Luciferase activity analysis of LIG1 transcriptional activity in GEM-resistant PDAC cells with or without hsa\_circ\_0007919 or FOXA1 or TET1 inhibition and with or without hsa\_circ\_0007919 or FOXA1 or TET1 overexpression. Data are the means  $\pm$  SDs (n = 3 independent experiments), \*\*  $p < 0.01$ , \*\*\*  $p < 0.001$

transcriptional activity of the *LIG1* promoter, while over-expressing *hsa\_circ\_0007919*, *FOXA1* or *TET1* enhanced *LIG1* transcriptional activity (Fig. 7H-I). These results revealed that *hsa\_circ\_0007919* enhances the transcription of *LIG1* by binding to *FOXA1* and *TET1*.

#### Gemcitabine induces *hsa\_circ\_0007919* expression through enhancing QKI-mediated back-splicing

CircRNAs are generated by back-splicing of exons or introns of their host genes, *hsa\_circ\_0007919* is formed by the circularization of *ABR* exons 3–16 (Fig. 1D), and *hsa\_circ\_0007919* expression was found to be upregulated in GEM-resistant PDAC tissues and cells compared with normal PDAC tissues and cells (Figs. 1B and 2E). Studies have revealed that multiple proteins are involved in the process of back-splicing during circRNA synthesis. Among several well-recognized regulators, QKI and *FUS* were reported to enhance the formation of circRNAs, while *ADAR1* was reported to exert the opposite effect [22–24]. To investigate the reason for high *hsa\_circ\_0007919* expression, we analyzed the correlations between the expression of abovementioned proteins and that of *hsa\_circ\_0007919* in GEM-resistant PDAC tissues and found that QKI was positively correlated with the expression of *hsa\_circ\_0007919*, while *FUS* had a lower correlation and *ADAR1* was negatively correlated with *hsa\_circ\_0007919* expression (Fig. 8A, S5A-B). Therefore, we predicted that QKI could promote the formation of *hsa\_circ\_0007919*. We silenced QKI in GEM-resistant PDAC cells and found that the expression of *hsa\_circ\_0007919* was downregulated but the expression of the *hsa\_circ\_0007919* host gene *ABR* was unaffected (Fig. 8B-C, S5C-D); moreover, the expression of QKI showed no difference between normal PDAC cells and GEM-resistant PDAC cells (Fig. 8D-E). QKI was reported to interact with introns flanking circRNA-formed exons in its pre-mRNA. We designed primers of *ABR* introns 2 and 16 and found that QKI could bind to both of these introns in PDAC cells and that this interaction was enhanced in GEM-resistant PDAC cells (Fig. 8F-G). These results revealed that GEM promotes the formation of *hsa\_circ\_0007919* by enhancing the interaction between QKI and *hsa\_circ\_0007919*-flanking introns to promote *hsa\_circ\_0007919* back-splicing and circularization.

In summary, this study delineates the mechanisms by which GEM enhances QKI-mediated *hsa\_circ\_0007919* splicing and circularization and *hsa\_circ\_0007919* recruits *FOXA1* and *TET1* to modulate *LIG1* transcription and DNA damage repair pathways, which contribute to resistance to GEM-induced DNA damage and apoptosis in PDAC cells (Fig. 8H).

## Discussion

PDAC is one of the most aggressive and deadly malignancies and is expected to become the second leading cause of cancer-related death within a decade [2]. Although molecular mechanistic research and treatment methods for PDAC have progressed in recent decades, the 5-year survival rate of PDAC is still the lowest among all malignant tumors due to reasons including chemoresistance [25]. CircRNAs are a class of noncoding RNAs and have been identified to be involved in multiple steps in tumor development, *PTK2* exon-derived *hsa\_circ\_0005273* promotes the proliferation and metastasis of BC cells by binding to miR-200a-3p to upregulate *YAP1* expression and inhibit the Hippo pathway [26], and the interaction of circ-*GALNT16* with *p53* is enhanced to inhibit the proliferation and metastasis of colorectal cancer cells via the inhibition of Snp2-mediated hnRNPK desumoylation [27]. We mainly focused on the relationships between circRNAs and GEM resistance in PDAC. Three GEM-resistant PDAC and three GEM-sensitive PDAC tissues were collected from clinical surgical specimens for analysis of circRNA expression levels with a circRNA chip, and *hsa\_circ\_0007919* expression was found to be significantly increased in GEM-resistant PDAC tissues. *Hsa\_circ\_0007919* is located on chr17:953289–1,003,975, with a length of 1545 bp. We found that *hsa\_circ\_0007919* was highly expressed in GEM-resistant PDAC tissues and cells, and *hsa\_circ\_0007919* inhibited apoptosis and DNA damage induced by GEM treatment. It has been shown that *hsa\_circ\_0007919* is involved in the progression of ulcerative colitis and tuberculosis [28, 29], and the current study suggests that *hsa\_circ\_0007919* plays an important role in GEM resistance in PDAC.

The predominant cancer treatments, other than surgery, are radiation and chemotherapy, which act by inducing DNA damage [30]. GEM is a common drug used in clinical chemotherapy for PDAC and usually acts by inducing SSBs [8], and a DSB can be formed when two SSBs are located near each other or when the DNA replication apparatus encounters SSBs, while DSBs are difficult to repair and extremely toxic [31]. To combat the hazard posed by DNA damage, cancer cells have evolved mechanisms called DDR pathways to facilitate DNA damage repair [32]. Among the components of these pathways, *LIG1*, a DNA ligase, completes the repair of almost all types of DNA damage by religating the broken phosphodiester skeleton in DSBs [33]. In addition, genetic deletion or low expression of *LIG1* was found to be associated with selective carboplatin resistance in pre-clinical models of triple-negative breast cancer (TNBC) [34]. *LIG1* deletion in ovarian cancer (OC) cells increased platinum cytotoxicity, which was associated with the accumulation of DSBs, S-phase arrest and increased proportions of apoptotic cells [19]. We performed RNA-seq

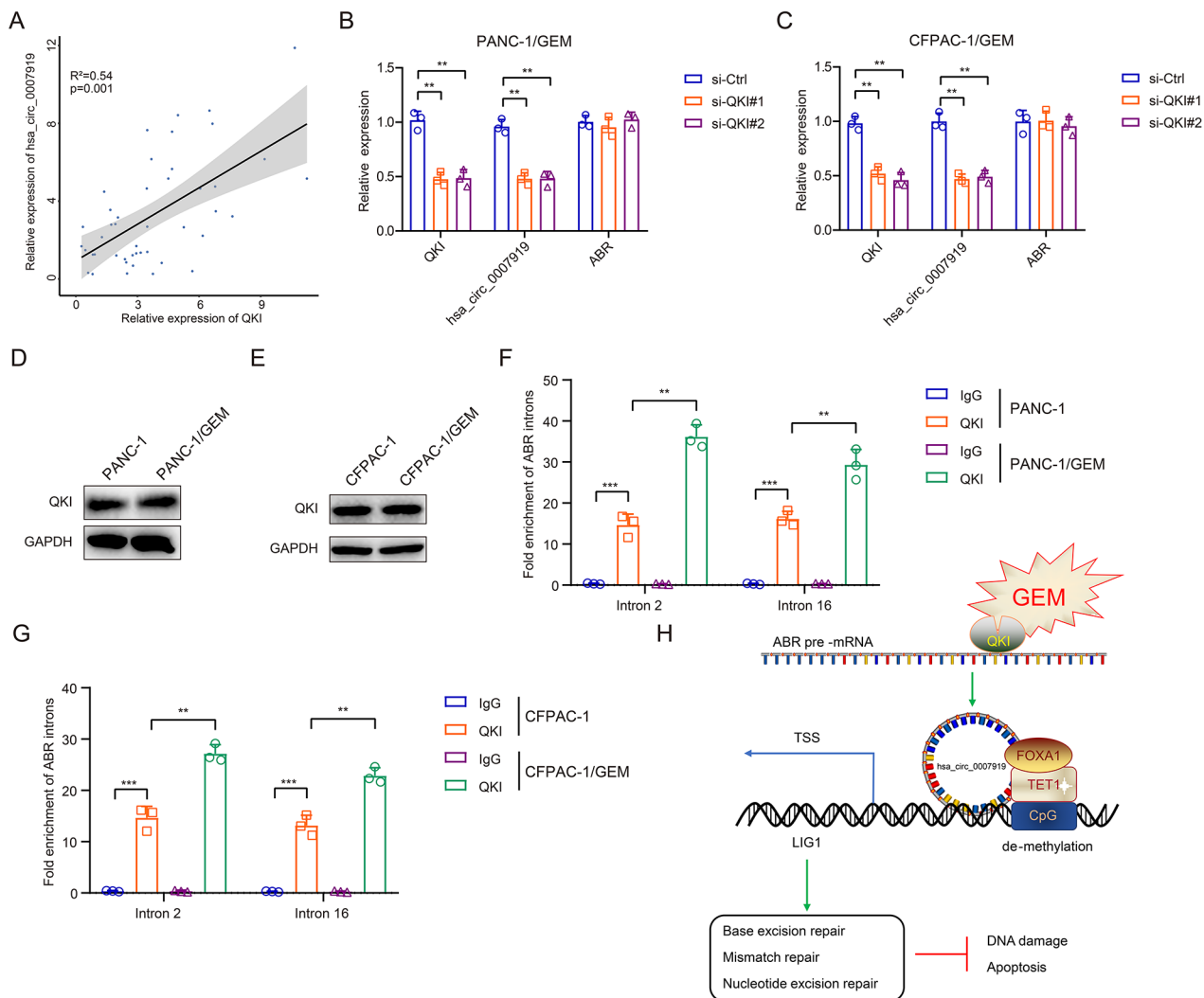


**Fig. 8** Gemcitabine induces *hsa\_circ\_0007919* expression through enhancing QKI-mediated back-splicing **(A)** Correlation analysis of QKI and *hsa\_circ\_0007919* expression in GEM-resistant PDAC tissues. **(B-C)** Expression of *hsa\_circ\_0007919* and ABR in GEM-resistant PDAC cells with or without QKI inhibition. **(D-E)** Expression of QKI in normal and GEM-resistant PDAC cells. **(F-G)** RIP assay analysis of the interaction between QKI and introns of ABR pre-mRNA in normal and GEM-resistant PDAC cells. **(H)** Schematic representation showing that GEM enhances interaction between QKI and ABR pre-mRNA and promotes back-splicing and cyclization of *hsa\_circ\_0007919*. Highly expressed *hsa\_circ\_0007919* recruits FOXA1 and TET1 to mediate de-methylation and transcription of LIG1 and upregulates the expression of LIG1. Overexpression of LIG1 activates base excision repair, mismatch repair and nucleotide excision repair pathways to inhibit the DNA damage and apoptosis of GEM-resistant PDAC cells. Data are the means  $\pm$  SDs ( $n = 3$  independent experiments), \*\*  $p < 0.01$ , \*\*\*  $p < 0.001$

analysis in control and *hsa\_circ\_0007919*-silenced GEM-resistant PDAC cells, and KEGG enrichment analysis and GSEA were performed on the identified differentially expressed genes. The results indicated that base excision repair, mismatch repair and nucleotide excision repair were the top-ranked enriched pathways, and LIG1 was enriched in all three DNA damage repair pathways. Here, we found that silencing *hsa\_circ\_0007919* decreased LIG1 expression and inhibited LIG1-mediated multiple DNA damage repair pathways to develop resistant to GEM in GEM-resistant PDAC cells. These results

indicate that *hsa\_circ\_0007919* could be a potential therapeutic target for GEM-resistant PDAC treatment.

FOXA1 is a member of the Forkhead Box protein family that is involved in cell growth and differentiation and is also a DNA binding protein involved in transcription and DNA repair [35]. Many members of the Forkhead Box protein family are associated with pancreatic metabolism and differentiation and the development of pancreatic cancer (PC), FOXO1 inhibition can mimic  $\beta$ -cell differentiation by downregulating  $\beta$ -cell-specific transcription and lead to abnormal expression of progenitor genes and the  $\alpha$ -cell marker glucagon [36]. FOXD1

directly promotes the transcription of SLC2A1 and inhibits the degradation of SLC2A1 through the RNA-induced silencing complex, thus promoting aerobic glycolysis in PC cells and enhancing their proliferation and metastasis [37]. Meanwhile, FOXA1 was reported to be associated with multiple kinds of cancers, especially prostate cancer (PCa) and BC. FOXA1 contributes to the activation of androgen receptor (AR) signaling that drives the growth and survival of PCa cells through direct interaction with AR and also has an AR-independent role in regulating epithelial-mesenchymal transition (EMT)[38], FOXA1 binds to the DNA-binding domain of STAT2 and inhibits STAT2 DNA-binding activity, IFN signaling gene expression and the tumor immune response in PCa and BC [39]. In addition to the binding of transcription factors to DNA promoter regions, methylation of DNA promoter regions also plays an important role in gene expression regulation, with hypermethylation of most gene promoter regions leading to reduced transcription levels [40]. TET1, a DNA demethylase, maintains genomic methylation homeostasis and accomplishes epigenetic regulation, which affect stem cells, immune responses and various malignant tumors [41]. TET1 promotes the transcription of CHL1 by binding to and demethylating the CHL1 promoter, thereby inhibiting the Hedgehog pathway, inhibiting EMT and sensitizing PDAC cells to 5-FU and GEM [42]. However, the role of FOXA1 and TET1 on GEM resistance in PDAC remains unknown. Here, we found that FOXA1 and TET1 can both bind to the promoter of LIG1 and that TET1 mediates demethylation of the LIG1 promoter and enhances FOXA1-mediated transcription of LIG1. It has been reported that FOXA2, a transcription factor precursor, was required for the regulation of pancreatic endoderm development, and TET1 deletion results in significant changes in FOXA2 binding in pancreatic progenitor cells. Loci with reduced FOXA2 binding have a low level of active chromatin modification and enrichment of bHLH motifs, resulting in functional  $\beta$ -cell defects [43]. In this study, we also confirmed that TET1 could increase the transcriptional activity of FOXA1 in GEM-resistant PDAC cells, which similar to the interaction between TET1 and FOXA2. These results enriched the further understanding of the interaction between DNA demethylase and transcription factors and the synergistic effect of transcriptional regulation.

CircRNAs are generated by back-splicing of pre-mRNAs produced by transcription of host genes, and cis-regulatory elements, trans-acting factors, RNA binding proteins (RBPs) and other related molecules can regulate the splicing and circularization of circRNAs [44]. Among these regulatory factors, QKI belongs to the STAR family containing KH domain RNA-binding proteins and has been found to affect pre-mRNA splicing, and QKI binds up- and down-stream of the circRNA-forming exons in

SMARCA5 to promote circRNA formation [45]. FUS is a member of the FET protein family and is reported to be a regulator of circRNA biogenesis; CircROBO1 upregulates KLF5 by sponging miR-217-5p, enabling KLF5 to activate FUS transcription and promote circROBO1 back-splicing, forming a positive feedback loop to enhance BC-derived liver metastasis [46]. ADAR1 is a member of the ADAR enzyme family that facilitates A-to-I editing of RNAs, circNEIL3 can inhibit ADAR1 expression by inducing GLI1 RNA editing through sponging miR-432-5p, and ADAR1 inhibition increases circNEIL3 expression to promote EMT and cell cycle progression in PDAC [47]. We found that GEM treatment enhances the interaction between QKI and introns 2 and 16 of ABR pre-mRNA to promote the splicing and circularization of hsa\_circ\_0007919. These results suggest that GEM treatment situation could enhance the function of QKI without changing its expression, which indicates a critical adaptation mechanism to developing resistance to GEM or other chemotherapy agents.

Taken together, our findings indicate that hsa\_circ\_0007919 can promote DNA damage repair to confront GEM treatment. Mechanistically, hsa\_circ\_0007919 recruits FOXA1 and TET1 to promote LIG1 transcription and activates the base excision repair, mismatch repair and nucleotide excision repair pathways to ameliorate the DNA damage and suppress the apoptosis induced by GEM. Furthermore, GEM treatment-enhanced interaction between QKI and ABR pre-mRNA led to increased biogenesis of hsa\_circ\_0007919 in a back-splicing-dependent manner. Our findings could be helpful for understanding the mechanism of GEM resistance and developing therapeutic strategies for chemotherapy-resistant PDAC.

#### Abbreviations

circRNA	Circular RNA
GEM	Gemcitabine
PDAC	Pancreatic ductal adenocarcinoma
OS	Overall survival
DFS	Disease-free survival
DDR	DNA damage response
5-FU	5-fluorouracil
BC	Breast cancer
FBS	Fetal Bovine Serum
IF	Immunofluorescence
BSA	Bovine Serum Albumin
IHC	Immunohistochemical
GSEA	Gene set enrichment analysis
FISH	Fluorescence in situ hybridization
ChIRP	Chromatin Isolation by RNA Purification
Co-IP	Co-immunoprecipitation
RIP	RNA binding protein immunoprecipitation
ChIP	Chromatin immunoprecipitation
MS-PCR	Methylation-specific PCR
SD	Standard deviation
SSB	Single-strand break
DSB	Double-strand break
TNBC	Triple-negative breast cancer
OC	Ovarian cancer

PC	Pancreatic cancer
PCa	Prostate cancer
AR	Androgen receptors
EMT	Epithelial-interstitial transition
RBP	RNA binding protein

## Supplementary Information

The online version contains supplementary material available at <https://doi.org/10.1186/s12943-023-01887-8>.

Supplementary Material 1  
Supplementary Material 2  
Supplementary Material 3  
Supplementary Material 4  
Supplementary Material 5

## Acknowledgements

We thank BGI for providing RNA-seq and data analysis, and we also thank AJE for language editing.

## Authors' contributions

XL, MX and ZXZ: conceptualization, methodology, investigation, writing original draft, visualization. GS, WN, ZC and ZY: data curation, validation, investigation, formal analysis. ZP, FXY, GJX and ZMM: software, investigation. RZQ: project administration, supervision. ZPB: supervision, resources, writing review & editing. All authors reviewed the manuscript.

## Funding

This research was supported by Science and Technology Project of Xuzhou Municipal Health Commission (XWKYHT20220152) and Xuzhou Medical University Affiliated Hospital Development Fund (XYFY2021017).

## Data availability

The data generated in this study are available upon request from the corresponding author.

## Declarations

### Ethics approval and consent to participate

This study was performed according to the ethical standards of Declaration of Helsinki and was approved by the ethics committee of the Xuzhou Medical University. All animal experiments were approved by the Animal Care Committee of Xuzhou Medical University.

### Consent for publication

We have obtained consents to publish this paper from all the participants of this study.

### Conflict of interest

The authors declare no potential conflicts of interest.

### Author details

- Department of General Surgery, Affiliated Hospital of Xuzhou Medical University, Xuzhou, China
- Institute of Digestive Diseases, Xuzhou Medical University, Xuzhou, China
- Shandong First Medical University and Shandong Academy of Medical Sciences, Shandong Cancer Hospital and Institute, Jinan, China
- Department of General Surgery, Xuzhou First People's Hospital, Xuzhou, China
- Department of General Surgery, Shangqiu Municipal Hospital, Shangqiu, China

Received: 3 June 2023 / Accepted: 24 October 2023

Published online: 04 December 2023

## References

- Siegel RL, Miller KD, Fuchs HE, Jemal A. Cancer statistics, 2022. *Cancer J Clin.* 2022;72:7–33. <https://doi.org/10.3322/caac.21708>.
- Kindler HL. A glimmer of Hope for Pancreatic Cancer. *N Engl J Med.* 2018;379:2463–4. <https://doi.org/10.1056/NEJMe1813684>.
- Wood LD, Canto MI, Jaffee EM, Simeone DM. Pancreatic Cancer: Pathogenesis, screening, diagnosis, and treatment. *Gastroenterology.* 2022;163:386–402e381. <https://doi.org/10.1053/j.gastro.2022.03.056>.
- Macheret M, Halazonetis TD. DNA replication stress as a hallmark of cancer. *Annu Rev Pathol.* 2015;10:425–48. <https://doi.org/10.1146/annurev-pathol-012414-040424>.
- Chatterjee N, Walker GC. Mechanisms of DNA damage, repair, and mutagenesis. *Environ Mol Mutagen.* 2017;58:235–63. <https://doi.org/10.1002/em.22087>.
- Tubbs A, Nussenzweig A. Endogenous DNA damage as a source of genomic instability in Cancer. *Cell.* 2017;168:644–56. <https://doi.org/10.1016/j.cell.2017.01.002>.
- Basu AK. DNA damage, mutagenesis and Cancer. *Int J Mol Sci.* 2018;19. <https://doi.org/10.3390/ijms19040970>.
- Perkhofer L, et al. DNA damage repair as a target in Pancreatic cancer: state-of-the-art and future perspectives. *Gut.* 2021;70:606–17. <https://doi.org/10.1136/gutjnl-2019-319984>.
- Khoronenkova SV, Dianov GL. ATM prevents DSB formation by coordinating SSB repair and cell cycle progression. *Proc Natl Acad Sci USA.* 2015;112:3997–4002. <https://doi.org/10.1073/pnas.1416031112>.
- Dreyer SB, et al. Targeting DNA damage response and replication stress in Pancreatic Cancer. *Gastroenterology.* 2021;160:362–377e313. <https://doi.org/10.1053/j.gastro.2020.09.043>.
- Chen LL. The biogenesis and emerging roles of circular RNAs. *Nat Rev Mol Cell Biol.* 2016;17:205–11. <https://doi.org/10.1038/nrm.2015.32>.
- Ashwal-Fluss R, et al. circRNA biogenesis competes with pre-mRNA splicing. *Mol Cell.* 2014;56:55–66. <https://doi.org/10.1016/j.molcel.2014.08.019>.
- Kristensen LS, Jakobsen T, Hager H, Kjems J. The emerging roles of circRNAs in cancer and oncology. *Nat Rev Clin Oncol.* 2022;19:188–206. <https://doi.org/10.1038/s41571-021-00585-y>.
- Xu X, et al. CircRNA inhibits DNA damage repair by interacting with host gene. *Mol Cancer.* 2020;19:128. <https://doi.org/10.1186/s12943-020-01246-x>.
- Han D, et al. The Tumor-Suppressive Human circular RNA CircITCH sponges mir-330-5p to Ameliorate Doxorubicin-Induced Cardiotoxicity through Upregulating SIRT6, Survivin, and SERCA2a. *Circ Res.* 2020;127:e108–25. <https://doi.org/10.1161/circresaha.119.316061>.
- Zhou X, et al. Circ-MBOAT2 knockdown represses Tumor progression and glutamine catabolism by miR-433-3p/GOT1 axis in Pancreatic cancer. *J Experimental Clin cancer Research: CR.* 2021;40:124. <https://doi.org/10.1186/s13046-021-01894-x>.
- Hu C, et al. circFARP1 enables cancer-associated fibroblasts to promote gemcitabine resistance in Pancreatic cancer via the LIF/STAT3 axis. *Mol Cancer.* 2022;21. <https://doi.org/10.1186/s12943-022-01501-3>.
- De Dosso S, et al. Treatment landscape of metastatic Pancreatic cancer. *Cancer Treat Rev.* 2021;96:102180. <https://doi.org/10.1016/j.ctrv.2021.102180>.
- Ali R, et al. Ligase 1 is a predictor of platinum resistance and its blockade is synthetically lethal in XRCC1 deficient epithelial ovarian cancers. *Theranostics.* 2021;11:8350–61. <https://doi.org/10.7150/thno.51456>.
- Castaneda M, Hollander PD, Mani SA. Forkhead Box transcription factors: double-edged swords in Cancer. *Cancer Res.* 2022;82:2057–65. <https://doi.org/10.1158/0008-5472.Can-21-3371>.
- Deng S, et al. RNA m(6a) regulates transcription via DNA demethylation and chromatin accessibility. *Nat Genet.* 2022;54:1427–37. <https://doi.org/10.1038/s41588-022-01173-1>.
- Xi Y, et al. CircBCAR3 accelerates Esophageal cancer tumorigenesis and Metastasis via sponging miR-27a-3p. *Mol Cancer.* 2022;21:145. <https://doi.org/10.1186/s12943-022-01615-8>.
- He Z, et al. FUS/circ\_002136/miR-138-5p/SOX13 feedback loop regulates angiogenesis in Glioma. *J Experimental Clin cancer Research: CR.* 2019;38:65. <https://doi.org/10.1186/s13046-019-1065-7>.
- Shi L, et al. Circular RNA expression is suppressed by androgen receptor (AR)-regulated adenosine deaminase that acts on RNA (ADAR1) in human hepatocellular carcinoma. *Cell Death Dis.* 2017;8:e3171. <https://doi.org/10.1038/cddis.2017.556>.
- Rahib L, et al. Projecting cancer incidence and deaths to 2030: the unexpected burden of thyroid, liver, and pancreas cancers in the United

- States. *Cancer Res.* 2014;74:2913–21. <https://doi.org/10.1158/0008-5472.Can-14-0155>.
26. Wang X, et al. Hsa\_circ\_0005273 facilitates Breast cancer tumorigenesis by regulating YAP1-hippo signaling pathway. *J Experimental Clin cancer Research: CR.* 2021;40. <https://doi.org/10.1186/s13046-021-01830-z>.
  27. Peng C, et al. Circ-GALNT16 restrains Colorectal cancer progression by enhancing the SUMOylation of hnRNPK. *J Experimental Clin cancer Research: CR.* 2021;40:272. <https://doi.org/10.1186/s13046-021-02074-7>.
  28. Wang T, et al. Integrated analysis of circRNAs and mRNAs expression profile revealed the involvement of hsa\_circ\_0007919 in the pathogenesis of ulcerative Colitis. *J Gastroenterol.* 2019;54:804–18. <https://doi.org/10.1007/s00535-019-01585-7>.
  29. Yuan Q et al. Identification of Key CircRNAs Related to Pulmonary Tuberculosis Based on Bioinformatics Analysis. *BioMed research international* 2022, 1717784, <https://doi.org/10.1155/2022/1717784> (2022).
  30. Groelly FJ, Fawkes M, Dagg RA, Blackford AN, Tarsounas M. Targeting DNA damage response pathways in cancer. *Nat Rev Cancer.* 2023;23:78–94. <https://doi.org/10.1038/s41568-022-00535-5>.
  31. Jackson SP, Bartek J. The DNA-damage response in human biology and Disease. *Nature.* 2009;461:1071–8. <https://doi.org/10.1038/nature08467>.
  32. Padella A, et al. Targeting PARP proteins in acute Leukemia: DNA damage response inhibition and therapeutic strategies. *J Hematol Oncol.* 2022;15. <https://doi.org/10.1186/s13045-022-01228-0>.
  33. Sallmyr A, Rashid I, Bhandari SK, Naila T, Tomkinson AE. Human DNA ligases in replication and repair. *DNA Repair.* 2020;93:102908. <https://doi.org/10.1016/j.dnarep.2020.102908>.
  34. Anurag M, et al. Proteogenomic Markers of Chemotherapy Resistance and Response in Triple-negative Breast Cancer. *Cancer Discov.* 2022;12:2586–605. <https://doi.org/10.1158/2159-8290.Cd-22-0200>.
  35. Bernardo GM, Keri RA. FOXA1: a transcription factor with parallel functions in development and cancer. *Biosci Rep.* 2012;32:113–30. <https://doi.org/10.1042/bsr20110046>.
  36. Casteels T, et al. An inhibitor-mediated beta-cell dedifferentiation model reveals distinct roles for FoxO1 in glucagon repression and insulin maturation. *Mol Metabolism.* 2021;54:101329. <https://doi.org/10.1016/j.molmet.2021.101329>.
  37. Cai K, et al. FOXD1 facilitates Pancreatic cancer cell proliferation, invasion, and Metastasis by regulating GLUT1-mediated aerobic glycolysis. *Cell Death Dis.* 2022;13:765. <https://doi.org/10.1038/s41419-022-05213-w>.
  38. Teng M, Zhou S, Cai C, Lupien M, He HH. Pioneer of Prostate cancer: past, present and the future of FOXA1. *Protein Cell.* 2021;12:29–38. <https://doi.org/10.1007/s13238-020-00786-8>.
  39. He Y, et al. FOXA1 overexpression suppresses interferon signaling and immune response in cancer. *J Clin Investig.* 2021;131. <https://doi.org/10.1172/jci147025>.
  40. Moore LD, Le T, Fan G. DNA methylation and its basic function. *Neuropsychopharmacology: Official Publication of the American College of Neuropsychopharmacology.* 2013;38:23–38. <https://doi.org/10.1038/npp.2012.112>.
  41. Liu W, Wu G, Xiong F, Chen Y. Advances in the DNA methylation hydroxylase TET1. *Biomark Res.* 2021;9:76. <https://doi.org/10.1186/s40364-021-00331-7>.
  42. Li H, et al. TET1 downregulates epithelial-mesenchymal transition and chemoresistance in PDAC by demethylating CHL1 to inhibit the hedgehog signaling pathway. *Oncogene.* 2020;39:5825–38. <https://doi.org/10.1038/s41388-020-01407-8>.
  43. Li J, et al. TET1 dioxygenase is required for FOXA2-associated chromatin remodeling in pancreatic beta-cell differentiation. *Nat Commun.* 2022;13:3907. <https://doi.org/10.1038/s41467-022-31611-x>.
  44. Chen L, et al. The bioinformatics toolbox for circRNA discovery and analysis. *Brief Bioinform.* 2021;22:1706–28. <https://doi.org/10.1093/bib/bbaa001>.
  45. Conn SJ, et al. The RNA binding protein quaking regulates formation of circRNAs. *Cell.* 2015;160:1125–34. <https://doi.org/10.1016/j.cell.2015.02.014>.
  46. Wang Z, et al. The circROBO1/KLF5/FUS feedback loop regulates the liver Metastasis of Breast cancer by inhibiting the selective autophagy of afadin. *Mol Cancer.* 2022;21:29. <https://doi.org/10.1186/s12943-022-01498-9>.
  47. Shen P, et al. CircNEIL3 regulatory loop promotes pancreatic ductal adenocarcinoma progression via miRNA sponging and A-to-I RNA-editing. *Mol Cancer.* 2021;20. <https://doi.org/10.1186/s12943-021-01333-7>.

## Publisher's Note

Springer Nature remains neutral with regard to jurisdictional claims in published maps and institutional affiliations.